

Spatial-resolved velocity measurements of shear flows with a novel differential Doppler velocity profile sensor

by

Jürgen Czarske¹⁾, Lars Büttner¹⁾, Thorsten Razik¹⁾,
Harald Müller²⁾, Dietrich Dopheide²⁾, Stefan Becker³⁾ and Franz Durst³⁾

¹⁾ Laser Zentrum Hannover e.V. (LZH), Laser Metrology,
Hollerithallee 8, D-30419 Hannover, Germany
E-Mail cz@lzh.de

²⁾ Physikalisch-Technische Bundesanstalt (PTB), Laboratory 1.31,
Bundesallee 100, D-38116 Braunschweig, Germany

³⁾ Friedrich-Alexander-Universität Erlangen-Nürnberg, Lehrstuhl für Strömungsmechanik (LSTM),
Cauerstr. 4, D-91058 Erlangen, Germany

ABSTRACT

A measuring system based on a differential laser-Doppler velocimeter has been extended to determine one-dimensional velocity profiles of shear flows with a spatial resolution in the micrometer range. The principle of the realised velocity profile sensor is based on two-wavelength fringe systems with different gradients of their fringe spacings. After wavelength-sensitive detection two Doppler frequencies are determined, which yield the position as well as the velocity component of individual tracer particles.

Conventional one-point laser Doppler velocity measurements suffer from a poor spatial resolution defined by the size of the measurement volume. Strong gradients of flows can not be resolved. Also stationary flows have to be assumed, since a traversing is necessary. The profile sensor offers the advantage that no mechanical scanning is needed to obtain flow velocity profiles over a length of up to 5 mm. In the centre of the measurement volume a spatial resolution of 1.6 μm results. The velocity profile sensor thus provides a tool for highly spatially resolved measurements of shear flows with strong velocity gradients.

Shear flow measurements were performed at wind tunnels at PTB and LSTM. Figure 1 shows spatial-resolved velocity measurements of laminar shear flows in flat-plate boundary layers. A good agreement with the Blasius velocity profile was obtained. The velocity profile sensor can be applied for the measurement of instationary flows in pipes as well as for highly-resolved velocity profile measurements of flows in micro-channels or micro-nozzles.

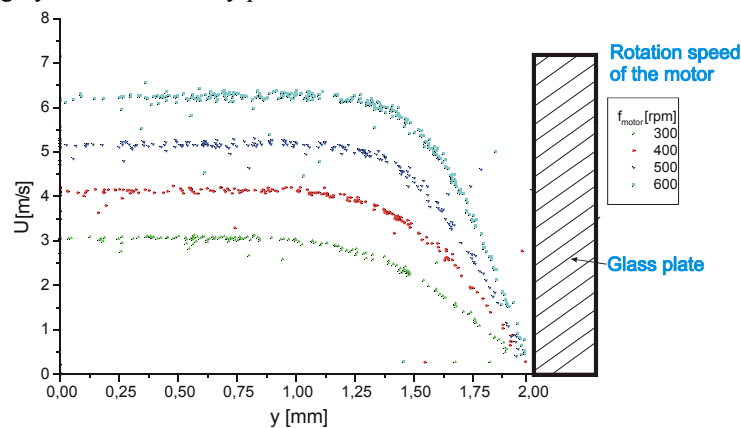


Figure 1: Spatial-resolved velocity measurement of laminar boundary layer flows close to a glass plate, placed into an Eiffel wind tunnel. Each data point represents one burst signal pair from individual particles moving through the measurement volume. Instantaneous measurements were accomplished for different free-stream velocities, corresponding to the rotation speed of a wind tunnel motor. The measurements were performed at the same position of $x = 25$ mm from the leading edge of the glass plate.

1. INTRODUCTION

Shear flows play an important role in practical developments as well as for fundamental studies. Since the tangential velocity drops to zero at the wall, a large velocity gradient is encountered in the boundary layer. The thickness of the boundary layer is scaled down with the free stream velocity, and is often in the sub-millimetre range. Thus the velocity profile has to be determined with a high spatial resolution. In the last few years, powerful numerical simulations of velocity fields became available. However, experimental verification is necessary, since numerical models are often not sufficient to describe the flow field. In small channels of micro-fluidic elements, the flow motion depends on surface interactions, which are difficult to simulate numerically (Meinhart et al 2000). Furthermore, the flow may be non-Newtonian, and complicated interactions between macromolecules, cells and walls can occur.

In general, optical methods offer a high spatial resolution due to their short wavelengths. CCD-camera-based laser measurement techniques are already well established. Particle image velocimetry (PIV) or particle-tracking velocimetry (PTV) can be used to obtain 2-D or also 3-D velocity data. PIV is based on a correlation of two images of scattering particle ensembles, recorded for a defined time interval by using two laser pulses. The spatial resolution depends on many factors, such as the particle size, the particle seeding density, the image quality of the optical system as well as the interrogation window of the correlation procedure used. Meinhart et al. have developed a micro-PIV/PTV-system with a spatial resolution of a few micrometers. Using polystyrene tracer particles of 200 nm diameter, velocity measurements were made in a boundary layer of about 20 μm thickness, occurring in a micro-channel flow with about 8 mm/s free stream velocity. The PIV technique requires direct imaging of an ensemble of particles. A high-resolving imaging system as well as sufficiently large tracer particles are necessary. Alternatively, velocity measurements can be accomplished by using the Doppler effect. Using iodine cells in order to convert a variation of the Doppler frequency into an optical intensity change, a continuous analogue velocity signal is yielded. Velocity fields can be determined by using CCD-cameras (Meyers 1995). This technique is referred to as Doppler global velocimetry (DGV) or planar Doppler velocimetry (PDV). A high spatial resolution is achieved, since velocity values are evaluated for each camera pixel. However, currently the velocity measurement accuracy is only approximately 0.5 m/s, mainly because of imperfections of the iodine cell, influences of the laser frequency jitter and disturbances due to reflections from model surfaces.

In contrast to, laser Doppler velocimetry (LDV) uses optical heterodyning of scattered light, enabling precise electronic determination of the Doppler frequency. Spatially high resolved LDV measurements have recently been achieved by using low-coherence light delivered by multi-mode fibres. A uniform fringe system inside a measurement volume of 40 μm length and 584 μm diameter was generated. It allows the determination of velocity gradients along the longitudinal axis of the measurement volume (Büttner et al 2001). Alternatively, a measurement length of 40 μm was achieved with Gaussian beams by using a microscope objective with a pinhole aperture in the LDV receiving optics (Mazumder et al 1981). This arrangement was employed to determine the local shear stress of turbulent flows. The skin friction coefficient is determined from the velocity gradient dU/dy at the wall. High measurement accuracy requires consideration of the transport properties of the tracer particles close to the wall as well as a further increase of the spatial resolution. Using short focal length lenses, a measurement volume of 5 μm x 5 μm x 10 μm was generated (Tieu et al 1995). The parabolic velocity profile of the laminar flow in a 175 μm thick micro-channel was measured. The measurement error, however, generally increases with scaling down the dimensions of the measurement volume. First the reduced number of fringes of the generated fringe system causes a systematic frequency measurement error of the fast Fourier transform (FFT) signal processing technique. Secondly, sharp focussing of the laser beams is encountered with increasing variation of the fringe spacing, which can be misinterpreted as turbulence intensity. Furthermore, it has to be recognised that LDV is a point-wise measurement technique, meaning that the velocity profile has to be scanned. This is time-consuming, and a stationary flow is required.

A fundamental novel principle is to evaluate the velocity of a flow field with spatial resolution. Strunck et. al. (1994, 1998) have presented a reference Doppler technique which achieves a spatial resolution of about $30\ \mu\text{m}$ along the y -axis of the measurement volume of almost $6\ \text{mm}$ length. Such a profile sensor was successfully applied for the spatial-resolved measurement of flows adjacent to a glass plate without the need for traversing the sensor. Limitations of this principle are given by the used reference Doppler technique, which is more difficult to align, and which yields lower accuracy than the differential Doppler technique usually employed.

This contribution presents a differential laser Doppler profile sensor for spatial resolved velocity measurements of shear flows, e.g. in boundary layers, figure 1. The advantages of this profile sensor can be outlined as follows:

- (i) A spatial resolution of about $1.6\ \mu\text{m}$,
- (ii) a relative velocity measurement error of about $1.4 \cdot 10^{-4}$ and
- (iii) distributed velocity measurements without traversing the sensor are achieved.

The drawbacks mentioned above concerning conventional point-wise LDA systems, such as strongly limited spatial resolution, systematic velocity measurement errors due to a non-correctable varying fringe spacing and the need for scanning the velocity profile can be overcome. The performance of the profile sensors demonstrates a significant progress compared to the former work (Czarske 2001), showing a spatial resolution of about $60\ \mu\text{m}$.

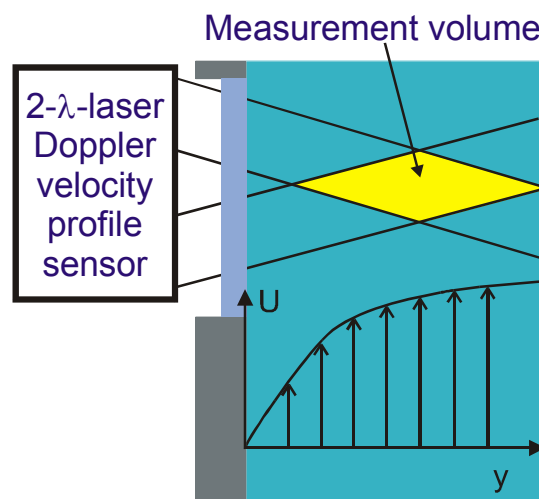


Figure 2: Scheme of spatial-resolving velocity measurements with a differential two-wavelength laser Doppler profile sensor.

2. LASER DOPPLER VELOCITY PROFILE SENSOR

The position as well as the velocity of individual tracer particles moving through the measurement volume are determined (Czarske 2001). Due to the statistical distributed particles the velocity profile of the flow is sequentially sampled. The y -position of the tracer particles is determined by the quotient of the Doppler frequencies f_1 and f_2 of the burst signals, resulting from the fringe systems of the laser wavelengths λ_1 and λ_2 :

$$q(y) = \frac{f_2(y, U)}{f_1(y, U)} = \frac{U(y)/d_2(y)}{U(y)/d_1(y)} = \frac{d_1(y)}{d_2(y)}, \quad (1)$$

where the Doppler frequency is given by $f_i = U/d_i$, ($i=1, 2$), with U as the x -component of the velocity. The fringe spacings d_i ($i=1, 2$) correspond to the two-colour fringe systems, generated in the same measurement volume.

Since the quotient of the frequencies is independent to the velocity, eq. (1), it allows to determine the y -position. By means of a calibration function ϕ , the position of the tracer particle is calculated according to $y = \phi[q(y)]$. An unambiguous measurement of the position requires a monotonic calibration function, which is achieved by opposite signs of the fringe spacing slopes.

The calculated y -position allows to determine the actual fringe spacings $d_1(y)$ and $d_2(y)$. Taking into account both measurements of the Doppler frequency, the arithmetic value of the velocity results in

$$U(y) = \frac{U_1(y) + U_2(y)}{2} = \frac{f_1(y, U) \cdot d_1(y) + f_2(y, U) \cdot d_2(y)}{2}. \quad (2)$$

In the differential Doppler technique, an interference fringe system in the measurement volume is generated by two coherent laser beams. Assuming ideal Gaussian beams with a beam quality factor of $M^2 = 1$, the variation of the fringe spacing $d(y)$ along the longitudinal y -axis of the measurement volume is formulated as

$$d(y) = \frac{\lambda}{2 \cdot \sin \Theta} \left(1 + \frac{y \cdot (\cos^2 \Theta) \cdot (y \cdot \cos^2 \Theta - y_W)}{y_R^2 \cdot \cos^2 \Theta - y_W (y \cdot \cos^2 \Theta - y_W)} \right), \quad (3)$$

where λ is the optical wavelength, Θ is the intersection half angle, y_W is the waist position relative to the crossing point of the beams, which is the centre of the measurement volume, $y_R = \pi w_0^2 / \lambda$ is the Rayleigh length, with w_0 as the $1/e^2$ radius of the intensity profile of the beam waist (Miles et al 1996). Different gradients $\partial d / \partial y$, ($i=1, 2$) of the fringe spacings can be obtained if the beam waist positions y_{W_i} , ($i=1, 2$) are longitudinally shifted against each other.

In figure 2, the set-up of the differential Doppler profile sensor is illustrated. Two laser diodes with an transversal single-mode power of 45 mW @ 660 nm and of 70 mW @ 785 nm, respectively, were used. The laser beams were collimated with aspherical lenses, and combined by a dichroic beam splitter. The laser beams were focussed onto a binary phase diffraction grating of 10 μm period. Using the ± 1 -diffraction orders, two coherent beams for each laser wavelength were obtained. The other diffraction orders were blocked by beam stops, figure 2. Using the arrangement of a Kepler telescope with two achromatic lenses of 60 mm focal length, the resulting four laser beams were imaged into the measurement volume. About half of the laser power was obtained in the measurement volume. The loss is caused by other diffraction orders of the grating and reflections at the optical interfaces.

Compared to half-reflecting mirrors, which are conventionally employed as beam splitters, grating beam splitters require lower alignment efforts, and the light polarisation can be chosen arbitrarily. Since the grating structure is imaged into the measurement volume, the interference fringe system is formed directly. Path length differences of the interfering laser beams are negligible. Thus, light sources with low coherence lengths can be employed easily. Furthermore, grating beam splitters are well-suited for a miniaturisation of the laser Doppler system (Czarske 2001).

Seeded tracer particles moving through the measurement volume scatter the laser light, which was then launched into a multi-mode fibre of 400 μm diameter. A forward- as well as backward-scattering arrangement can be used. By means of a dichroic beam splitter the scattered light was separated and then focussed to two avalanche photo-diodes (APD), figure 2. After amplification an analogue-to-digital conversion and storing was accomplished with a 14 bit data acquisition PC card, model Gage CompuScope 1450. The signal spectra were calculated by means of the FFT technique, implemented by the software LabVIEW. By an interpolation procedure the centre frequencies of the obtained single spectral lines were determined.

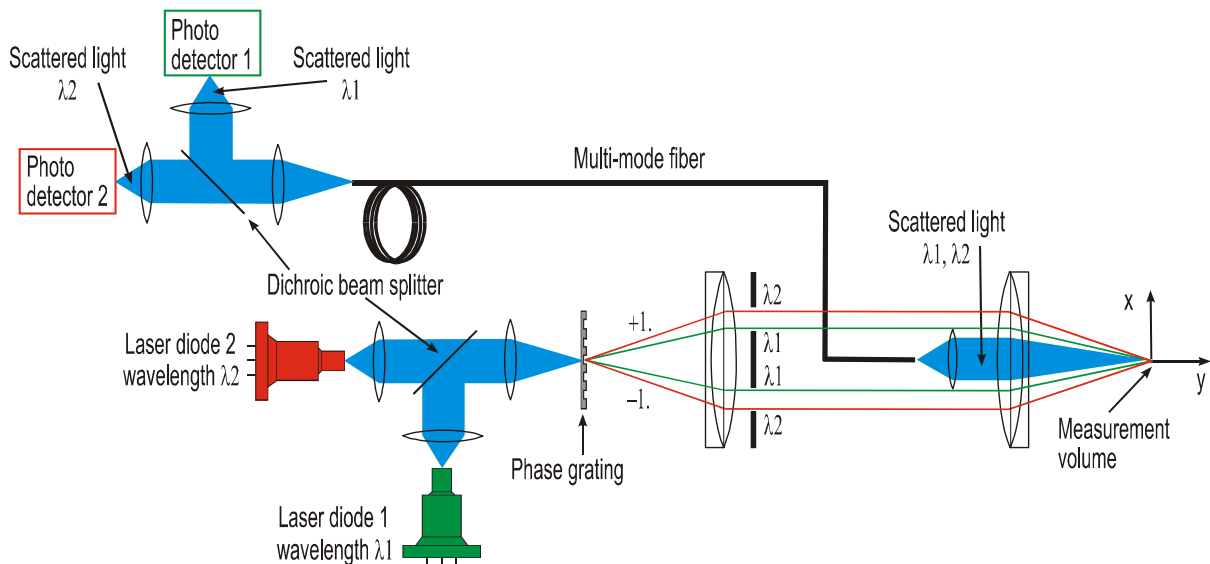


Figure 3: Arrangement of the differential laser Doppler profile sensor (channel 1: $\lambda_1=660$ nm, channel 2: $\lambda_2=785$ nm).

Different gradients of the fringe spacings $\partial d_i / \partial y$, ($i=1, 2$) were generated by adjusting the beam waists to be located on opposite sides of the measurement volume. A difference between the waist positions of about 20.9 mm was obtained. Besides good separation of the beam waists, the concept of the sensor requires an overlapping of the fringe systems, in order to allow simultaneous measurements of the Doppler frequencies. For this reason, achromatic doublet lenses were employed.

Figure 3 shows the determined fringe spacings along the y-axis for both laser wavelengths. In the centre of the measurement volume both fringe systems have the same spacing of 5.1 μm . In this plane the fringes can be considered as an image of the grating. Assuming geometrical optics, the fringe spacing results as $d = \frac{1}{2} g \beta = 5 \mu\text{m}$, with the grating constant $g = 10 \mu\text{m}$ and the wavelength-independent magnification factor $\beta = f_2 / f_1 = 1$, with the

focal lengths $f_1 = f_2 = 60 \text{ mm}$ of the achromatic imaging lenses. Outside of the imaging plane, the change of the fringe spacings correspond to the varying curvature of the wavefronts of the Gaussian beams. An opposite variation of the spacings was achieved due to the separation of the Gaussian beam waists to opposite sides of the measurement volume. It results a monotonic function of the quotient $q(y)$ of the fringe spacings, figure 4. This calibration curve ensures an unambiguous measurement of the tracer particle position within the entire measurement volume of 5 mm length. Relative to the centre of the measurement volume, a variation of the quotient of -33% c.f. 82% was obtained, figure 6. In the former work (Czarske 2001), the variation of the quotient was only -4% , c.f. $+4\%$. As a consequence, the measurement error of the position is reduced significantly with the actual arrangement.

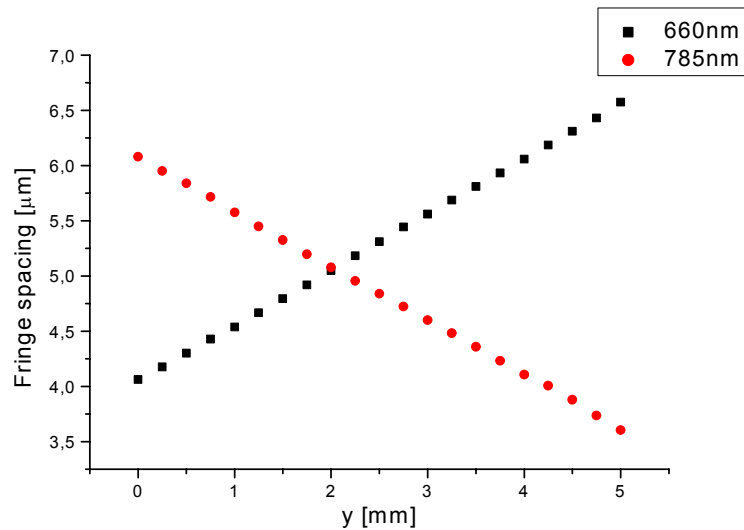


Figure 4: Fringe spacings d_1 and d_2 , corresponding to the laser wavelengths $\lambda_1=660 \text{ nm}$ and $\lambda_2=785 \text{ nm}$, versus the y -position of the measurement volume.

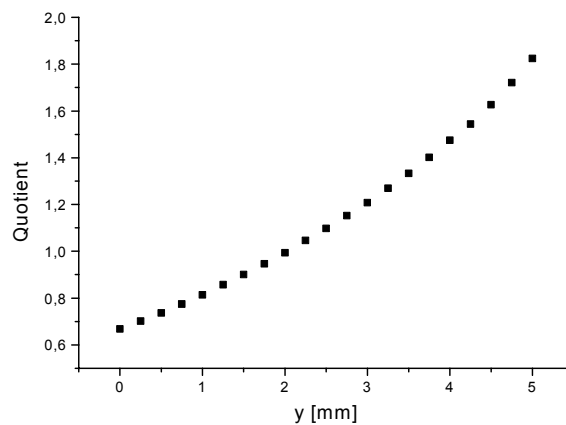


Figure 5: Calibration function of the profile sensor, described as the quotient of the fringe spacings $q=d_1/d_2$ versus the y -position.

The measurement error of the profile sensor is investigated experimentally. Dust particles with a spherical size of a few micrometers were used as scattering objects. They are onsite the surface of a cylindrical disc of BK7 glass, which was polished and has an average radius of 92.079 mm with a maximum variation of 7 μm . Figure 6 outlines the measurement error of the position of a single scattering particle, which is onsite the glass disc, rotating with a constant velocity. At each y-position of the disc the Doppler frequency measurements were repeated 20 times, enabling an accurate estimation of the standard deviation according to the t-distribution from Student. Close to the centre of the measurement volume an uncertainty of the measured position of $\Delta y \approx 1.6 \mu\text{m}$ is obtained. However, Figure 6 shows a systematic measurement error of about 4 μm in maximum. It can be reduced by an appropriate matched calibration curve.

At the boundaries of the measurement volume the statistical measurement error increases to about 4 μm , because of reduced signal quality due to smaller SNR, fewer number of signal periods and distortions of the signal shape. Over the entire measurement range of 5 mm an averaged spatial resolution of about 2.5 μm is obtained, i.e. the relative spatial resolution of the profile sensor is about 0.05%. It can be shown that the velocity measurement error depends on the obtained frequency accuracy only. The empirical measurement uncertainty results in $\Delta U / U \approx 1.4 \cdot 10^{-4}$. It demonstrates that the profile sensor exhibits a small virtual turbulence intensity.

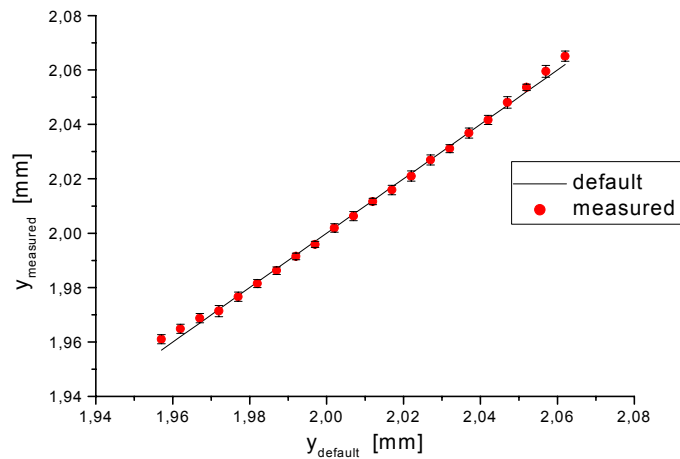


Figure 6: Measured positions versus default positions. A statistical measurement error of $\Delta y = 1.6 \mu\text{m}$ is obtained.

3. VELOCITY MEASUREMENTS OF FLAT-PLATE BOUNDARY LAYER FLOWS

The experimental verifications of the velocity profile sensor were carried out in an Eiffel wind tunnel at the PTB as well as a closed-loop wind tunnel at the LSTM. Liquid tracer particles (DEHS - diethylhexyl sebacate) with diameters of about $2.5 \mu\text{m}$ were seeded to the flow. The scattered light from the tracers were detected in forward direction. A free-stream flow was investigated first. Figure 7 shows the result of a spatial-resolved velocity measurement in the closed-loop wind tunnel. Slot-intervals of about $200 \mu\text{m}$ were used to calculate the mean velocity as well as the relative rms velocity fluctuation, i.e. turbulence intensity. Figure 7 outlines an uniformity of about 1.5% over a measurement length of about 3 mm. The averaged turbulence intensity is about 0.35%. It is in agreement with the referred turbulence intensity of lower than 0.4% (Durst et al 2001), determined with hot-wire technique.

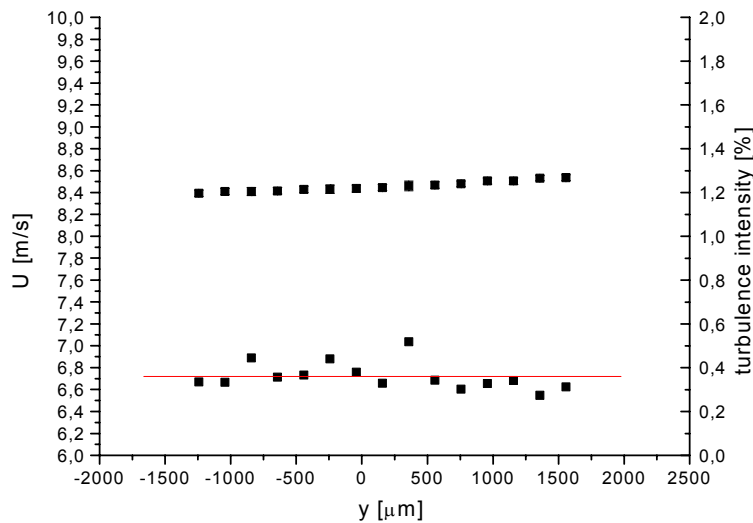


Figure 7: Mean velocity and turbulence intensity of the free-stream flow in a closed-loop wind tunnel.

For the measurement of boundary layer flows, a glass plate was introduced into the test section of the wind tunnel. A NACA profile of the leading edge of the plate was realised in order to ensure a laminar flow. The plate was aligned carefully to suppress pressure gradients along its x-direction. This complies with the requirements for a laminar Blasius boundary layer, if Reynolds numbers lower than about $Re_x \approx 3.5 \cdot 10^5$ occur (Schlichting 1987). The Reynolds number is defined as $Re_x = x U_\infty / \nu$, where x is related to the leading edge of the plate, U_∞ is the free-stream velocity and $\nu \approx 1.5 \cdot 10^{-5} \text{ m}^2/\text{s}$ is the kinematic viscosity of air. Velocity profile measurements were performed for different free stream velocities, figure 8. The maximum Reynolds number was $Re_x = 51 \text{ mm} \cdot 8.5 \text{ m/s} / (1.5 \cdot 10^{-5} \text{ m}^2/\text{s}) \approx 3 \cdot 10^4$, indicating a laminar flow (see above). Figure 9 shows the good agreement of the spatial-resolved velocity measurements with the theory from Blasius (Schlichting 1987).

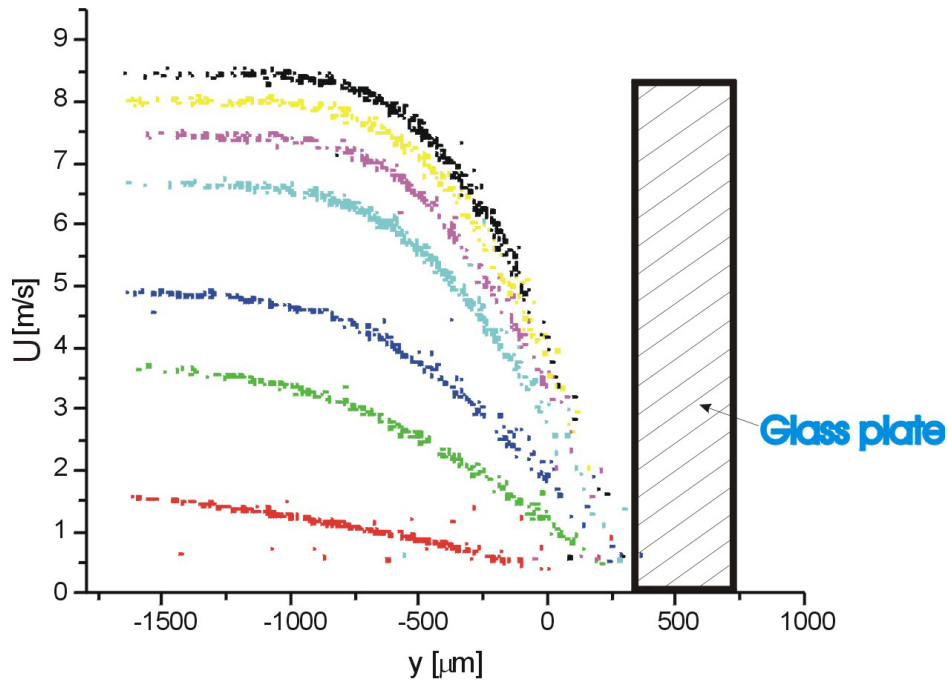


Figure 8: Instantaneous measurements of the velocity profile of a Blasius boundary layer flow. At the same position $x = 51$ mm downstream from the leading edge of the glass plate, spatial resolved velocity measurements were performed for different free-stream velocities of the close-loop wind tunnel. The non-slip condition of boundary layers, i.e. that the velocity drops to zero at the surface of the plate, was used to determine its absolute position, lying at $y \approx 0.35$ mm.

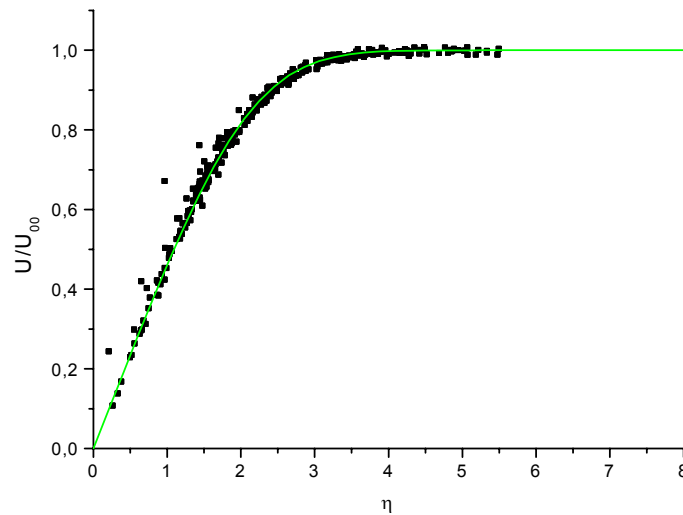


Figure 9: Measured velocity profile of a laminar boundary layer flow in normalised coordinates U/U_∞ and $\eta = y \sqrt{\frac{U_\infty}{2\nu x}}$ (position of $x = 41$ mm). The individual measurement results show a good coincidence with the theoretical curve (solid line) of a Blasius boundary layer.

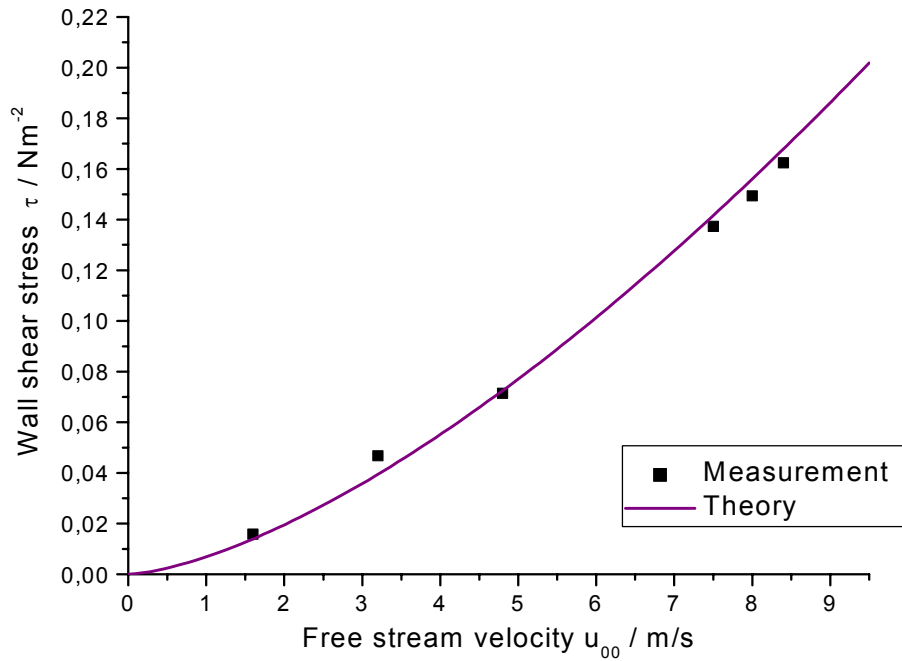


Figure 10: Measured wall shear stress for different free-stream velocities at the same position $x = 51\text{mm}$ downstream from the leading edge of the glass plate. A good agreement with the theory from Blasius is obtained.

One important motivation for the measurement of the velocity profile of flows adjacent to walls is the determination of the shear stress, which allows to calculate the skin friction drag (Durst et al 1996). The wall shear stress is given by

$$\tau_w = \mu \left. \frac{dU}{dy} \right|_{y=0}, \quad (4)$$

which is deduced from the gradient of the velocity profile $U(y)$ in the near-wall region, where $\mu = 1.8 \cdot 10^{-6} \text{ N s m}^{-2}$ is the dynamic viscosity of air, U is the velocity component parallel to the surface and y is the coordinate normal to the surface. The local wall shear stress of a laminar boundary layer results by equation (4) in:

$$\tau_w = \mu U_\infty \sqrt{\frac{U_\infty}{2\nu x}} f''(0) = 0.332 \mu U_\infty \sqrt{\frac{U_\infty}{2\nu x}} \quad (\text{Schlichting 1987}).$$

It should be remarked, that due to Blasius's resistance law the local skin friction coefficient is given by $c_f = \tau_w / (0.5 \rho U_\infty^2) = 0.664 \text{ Re}_x^{-0.5}$, where ρ represents the density of air. Figure 10 shows the calculated wall shear stress from the measured velocity profiles. The slope of the data close to the plate were evaluated according to equation (4). The comparison with the theoretical Blasius curve demonstrates a good coincidence.

4. CONCLUSIONS

A novel method to measure flow velocity profiles with a resolution in the micrometer range has been proposed. Compared to a conventional laser Doppler velocimeter (LDV) the velocity profile can be measured without traversing the LDV set-up. A spatial-resolved measurement of the position as well as the velocity of single tracer particles is performed inside the measurement volume. Over the measurement range of about 5 mm the entire boundary layer flow can be evaluated. In the centre of the measurement volume an uncertainty of about 1.6 μm results for the position measurement. The average spatial resolution in the entire measurement volume corresponds to about 2.5 μm . Thus, about 2000 different positions of single tracer particles can be discriminated. The spatial resolution can be further improved e.g. by increasing the signal-to-noise ratio of only around 5 dB currently.

Spatial-resolved velocity measurements of shear flows such as flat-plate boundary layer flows were performed. The obtained near-plate mean velocity data allows to determine the local wall shear stress, resulting in the skin friction drag. Since no traversing of the sensor is necessary, the instantaneous velocity profile of non-stationary flows in pipes can be monitored. By the velocity profile measurement of the outlet flow the flux of pipes or nozzles can be estimated.

Due to the high spatial resolution of the proposed profile sensor, measurements of thin boundary layers, e.g. of flows in micro-channels and injection nozzles, can be accomplished. The length of the measurement volume has to be adapted to the channel size of lower than 100 μm typically. It is expected that an enhancement of the position accuracy towards the submicrometer range can be reached. Applications are also seen in spatial-resolved velocity measurements of flows adjacent to air plane wings as well as free stream flows or spherical Couette flows, to refer some examples.

Acknowledgements: The authors wish to thank Mr. F. Bergonnier (NFIO, Orsay, France) for his excellent technical assistance at the experiments. Support by Mr. H. Lienhart, Mr. E.-S. Zanon (both LSTM) and the members of Laboratory 1.31 of PTB is acknowledged. Dr. S. Günster (LZH) is thanked for manufacturing the dichroic beam splitters for multiplexing as well as demultiplexing of the two-colour beams. This research work was partially funded by the DFG.

REFERENCES

- Büttner L, Czarske J 2001 A multimode-fiber laser-Doppler anemometer for highly spatially-resolved velocity measurements using low coherence light, *Measurement Science and Technology*, 12, pp.1891-1903
- Czarske J 2001 Laser Doppler velocity profile sensor using a chromatic coding, *Measurement, Science and Technology*, 12, pp.52-57
- Durst F, Kikura H, Lekakis I, Jovanovic J, Ye Q 1996 Wall shear stress determination from near-wall mean velocity data in turbulent pipe and channel flows, *Exp. in Fluids*, 20, pp.417-428
- Durst F, Zanon ES, Pashtrapanska M 2001 In situ calibration of hot wires close to highly heat-conducting walls, *Experiments in Fluids*, 31, pp.103-110.

Mazumder MK, Wanchoo S, McLeod P C, Ballard G S, Mozumdar S and Caraballo N 1981 Skin friction drag measurements by LDV; *Appl. Opt.* 20, 2832–7

Meinhart CD, Wereley ST and Santiago JG 2000 Micron-resolution velocimetry techniques, (*Laser Techniques applied to fluid mechanics, selected papers from the 9th international symposium, Lisbon, Portugal, 13-16 July 1998*, Ed. R.J. Adrian et al. pp.57-70, paper I.4, Berlin: Springer)

Meyers JF 1995 Development of Doppler global velocimetry as a flow diagnostic tool, *Measurement Sci. & Technol.*, 6, pp.769-783.

Miles P and Witze P 1996 Evaluation of the Gaussian beam model for prediction of LDV fringe fields 8th Int. Symp.—Applications of Laser Techniques to Fluid Mechanics (Lisbon, 1996, ed R Adrian et al), paper 40.1

Schlichting H 1987 *Boundary layer theory* (McGraw-Hill, New York, USA)

Strunck V, Grosche G and Dopheide D 1994 Scanning laser Doppler probe for profile measurements, *Proc. 7th Int. Symp.—Applications of Laser Techniques to Fluid Mechanics* (Lisbon, 1994, ed R Adrian et al), paper 17.1

Strunck V, Müller H, Dopheide D 1998 Traversionsfreie LDA-Grenzschichtmessungen mit Mikrometerauflösung im Meßvolumen, 6th Conf. Lasermethoden in der Strömungsmeßtechnik (Essen, 28th-30th September 1998, ed. W. Merzkirch et al.) pp. 28.1-28.11 (in German)

Tieu AK, Mackenzie MR and Li EB 1995 Measurements in microscopic flow with a solid-state LDA, *Exp. Fluid*, Vol.19, pp.293-294.